Self-Limiting Aggregation Leads to Long-Lived Metastable Clusters in Colloidal Solutions

M. Meyer,* E. C. Le Ru,† and P. G. Etchegoin‡

The MacDiarmid Institute for Advanced Materials and Nanotechnology, School of Chemical and Physical Sciences, Victoria University of Wellington, P.O. Box 600 Wellington, New Zealand

Received: October 13, 2005; In Final Form: January 24, 2006

The existence of a metastable state with limited Coulomb-blocked aggregation at the onset of instability in a colloidal solution is proposed and demonstrated both experimentally and theoretically (through Monte Carlo simulations). Such a stable state of small clusters of metallic colloids happens to be extremely important for techniques such as surface-enhanced Raman scattering (SERS), which profits explicitly from collective plasmon resonances in these clusters to boost Raman signals of specific analytes. In fact, SERS provides a unique tool to understand, monitor, and study the onset of aggregation in colloidal silver/gold and to prove the existence of the proposed state at the boundary of colloid coalescence.

I. Introduction

A. Colloid Stability. One of the most remarkable properties of colloidal solutions[1] is that they actually exist. The equilibrium achieved in the steady state of a colloidal system is a fine balance between hard-core repulsions, van der Waals attractions, screened Coulomb interactions, and hydrodynamic forces (coupling through movement). The different roles, magnitudes, and relative strengths of these contributions produce an amazing variety of phenomena that go from glass formation to crystallization (used in opal photonic crystals for example[2]) to a long list of many-body phenomena, which have been covered extensively in the specialized literature.[3]

Even though the Derjaguin, Landau, Verwey, and Overbeek theory[4,5] (DLVO theory) of the colloidal state provides the basic framework for the understanding of colloidal stability/instability, and is well researched and studied, it is clear that the DLVO theory is, after all, a mean field approximation and does not necessarily explain some of the more subtle and interesting phenomena observed in colloids. In the past few years, there has been an increasing number of publications and authors dedicated to the study of colloid stability beyond the DLVO theory, with particular emphasis on the perturbing effects of boundaries[6,7] and many-body effects.[8,9] The increasing number of anomalous situations seen experimentally (like colloids of the same charge sign attracting each other in situations where the DLVO theory would predict repulsion[10]) has increased the interest for previously overlooked aspects of colloidal dynamics.

Of particular importance for this paper is the *onset of instability* of a charge-stabilized colloidal solution; that is, the condition that separates a stable colloid from aggregation by screening of the repulsive Coulomb barrier through the ionic content of the solution. It is well known that silver colloidal solutions are not thermodynamically stable. Their long-term stability is usually obtained by the presence of surface charges (usually negative). The strong Coulomb repulsion then provides a large potential barrier, V_{max}, preventing two colloids from aggregating, which leads to a metastable solution of single colloidal particles (typically for $V_{max} > 15\ k_BT$). This Coulombic repulsion can be screened by addition of an electrolyte. Above the so-called critical coagulation concentration (c.c.c), the Coulombic force no longer dominates the van der Waals attraction ($V_{max} < 0$) and this results in rapid coagulation of all of the colloids into very large aggregates. We here focus on the intermediate situation, $0 < V_{max} < 15\ k_BT$, where a barrier still exists, but is not large enough to ensure a long-lived metastable state of *single* colloidal particles. We will argue that there is experimental and theoretical evidence for a metastable state with self-limiting aggregation dynamics in which small clusters are formed and then further aggregation is prevented by Coulomb blocking. This creates a long-lived metastable state of small clusters in the liquid, which happens to be extremely important for certain types of spectroscopy like surface-enhanced Raman scattering (SERS). From the viewpoint of colloid physics, therefore, we are interested in what happens at the boundary of instability and, in particular, the dynamics and statistics of the aggregation process.

Notwithstanding, the problem can be formulated backward in terms of its importance for SERS[11] and any other type of spectroscopy that profits from collective plasmon resonances in small metallic clusters in liquids. There is actually a link between the two aspects, and this is presented briefly in the next subsection.

B. Surface-Enhanced Raman Scattering. Discovered in 1974,[12−14] SERS allows highly sensitive spectroscopy[15,16] due to Raman enhancement factors in the range 10^5-10^{14}. The magnitude of the enhancement is large enough in many cases to allow single-molecule Raman spectroscopy.[17,18] Clearly, the key issue of this discussion is the physical origin of the Raman enhancement itself which, like in the colloid stability problem, is still not resolved to a satisfying extent despite the fact that the basic principles have been known for a very long time[15,16] and are basically understood.

It is widely accepted that next to a minor chemical component the electromagnetic (EM) enhancements, caused by localized surface plasmon excitations, account for most of the signal seen in SERS. Furthermore, it is known that the EM-field in the near environment of a metal nanoparticle is amplified nonuniformly causing, in particular, the so-called *hot spots* on the particle surface, which depend on a long list of conditions including

* Corresponding author. E-mail: kiwimatto@gmail.com.
† E-mail: Eric.LeRu@vuw.ac.nz.
‡ E-mail: Pablo.Etchegoin@vuw.ac.nz.

10.1021/jp055866b CCC: $33.50
Published on Web 03/04/2006

geometry, orientation with respect to polarization, wavelength, and so forth.

Hot spots profit from plasmon−plasmon interactions among particles. Even the simplest types of aggregates show EM enhancements that are several orders of magnitude higher than those at the surface of a single particle. Calculated EM enhancements obtained from various approximations in dimers or higher aggregates of metal particles can explain the observed Raman enhancements to a large extent. The so-called *activation* of colloidal solutions in SERS, which is nothing but the introduction of a salt (typically KCl or NaCl) to initiate aggregation and boost Raman signals, profits directly from the (red-shifted) collective plasmon resonances present in the aggregates.[19,20] However, this approach in general leads to unstable solutions, which lose their activity within a few hours. This affects the reproducibility and interpretation of such SERS experiments and emphasizes the importance of stable solutions of small clusters for SERS.

From this brief introduction, it is clear that we have in SERS a technique with an extremely high sensitivity to the presence of small clusters of colloids and, accordingly, a technique that is tailor-made to study the initial stages of aggregation very close to the instability threshold. In what follows, we shall show that SERS provides unique evidence for some phenomena that would not be observable otherwise.

C. SERS and Colloidal Stability. Massive SERS enhancements can only come from aggregated clusters. Both the experimental and theoretical evidence for this are overwhelming and will be further reaffirmed in the Experimental Section. The conventional picture in colloidal dynamics is that once aggregation has started the process continues to its inevitable outcome, which is the aggregation of clusters that become too large to survive in solution by buoyancy. The dynamics of dimer, trimer, tetramer, and so forth, formation is described as a textbook example of colloidal instability in most advanced books on the subject.[1]

Some of these conclusions seem to be in flagrant contradiction with what we have observed in SERS active liquids. If the original colloidal solution is mixed with a small quantity of a SERS active dye, then extremely weak Raman signals are observed. This is the *single-particle enhancement* regime, which shows that large enhancements can only be achieved by aggregation. However, the instability threshold introduced by adding a salt can be measured to a relatively high accuracy within a few millimoles in concentration. If we now prepare a sample with the dye and a salt concentration very close (but below) the instability threshold, then what we observe is a boost of the Raman signals in SERS by several orders of magnitude. This implies that aggregation has started; we can monitor the beginning of this process with extremely high sensitivity because of the efficiency of SERS.

At first glance, this would suggest that the aggregation process has started because the Coulomb barrier of the colloids has been screened, and there is nothing now stopping the system from continuing the aggregation process until the clusters collapse by gravitational effects. As will be shown, this is *not* what is observed experimentally. Some of these SERS active solutions, where limited aggregation has obviously occurred, remain active at the same level without any loss of signal for many months (10 months is the longest evidence we have at the moment) and, therefore, this suggests the presence of a long-lived state with limited aggregation right at the boundary of instability. We demonstrate here the experimental and theoretical evidence for such a state and argue in favor of a specific mechanism for it to happen.

This brings us back, in fact, to the origins of SERS signals in colloidal fluids, a much debated subject in the SERS literature because of its relevance in single-molecule detection. To understand what we believe is self-limiting aggregation by Coulomb-blocking, which comes as a many-body effect in this context, we need to review briefly the DLVO potential and its main characteristics for the specific colloidal fluids we use. We will then be able to highlight the importance of this metastable state for both the study of the dynamics of aggregation in colloid science on one hand, and SERS on the other.

II. DLVO Interaction Potential

In the 1940s Derjaguin, Landau, Verwey, and Overbeek[4,5] developed a general theory (DLVO theory) to solve the electrostatics problem of an electrolyte with charged boundaries. This theory in its simplest form gives an approximation of the positive interaction potential corresponding to the repulsive behavior of charged particles within an ionic solution. This is then added to the (negative) interaction potential for van der Waals attraction to form the total DLVO interaction potential for a pair of colloids. Although some of these approximations may not always be valid, this theory provides a simple and general approach, which has been shown to agree qualitatively and semiquantitavely with observations in many cases. For these reasons, it has been used frequently in the past to describe colloid dynamics and aggregation effects. One feature of the DLVO theory is it simplifies the Poisson−Boltzmann equation by expanding the Boltzmann factor (which depends on the ion density) into a power series that is truncated after the first-order term (linear approximation). The DLVO interaction potential with this screened Coulomb repulsion (for two identical spheres) then reads

$$\frac{U(r)}{k_B T} = \frac{e^2 Z^2}{4\pi\epsilon k_B T}\left[\frac{e^{\kappa a}}{1+\kappa a}\right]^2 \frac{e^{-\kappa r}}{r} + \frac{V(r)}{k_B T} \qquad (1)$$

where r is the center-to-center separation of spheres of radius a with charges Z. κ^{-1} is the Debye−Hückel screening length of the electrolyte, which can be calculated from the concentrations n_j and charges z_j of the involved ions by

$$\kappa^2 = \frac{e^2}{\epsilon\, k_B T}\sum_{j=1}^{N} n_j z_j^2 \qquad (2)$$

All of the other symbols have the standard meaning. The exponential decay of the potential is a result of the screening.

The second component of the total effective potential is the *van der Waals* interaction $V(r)$ (normalized by $k_B T$), which accounts for the attraction between two spheres of radii a and can be approximated by[3]

$$\frac{V(r)}{k_B T} = -\frac{A_{\text{eff}}}{6 k_B T}\left[\frac{2a^2}{r^2-4a^2} + \frac{2a^2}{r^2} + \ln\left(1-\frac{4a^2}{r^2}\right)\right] \qquad (3)$$

where A_{eff} is the Hamaker constant, which depends on the materials of the objects under consideration and on the medium they are immersed in (see ref 21).

The practical application of this theory to experiments is not straightforward because some of the parameters (particularly A_{eff} and Z) in eq 1 and 3 are hard to obtain accurately. These values can, however, be adjusted so that they predict correctly the value of the critical coagulation concentration. Accordingly, the following values have to be considered as rough estimates for the real sample conditions (to be described later). For our

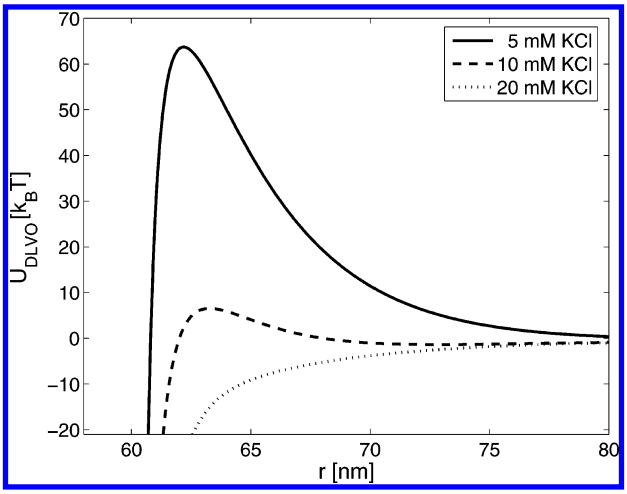

Figure 1. DLVO interaction potentials in solutions of different ionic (KCl) concentration (see legend) for Ag colloids. The following parameters were used in the calculation: radii $a = 30$ nm, $Z = 1000$, and $A_{eff}/k_BT = 60$. In this plot, a distance of 60 nm means that the two spherical colloids are touching each other. Note the development of a deep negative potential very close to the "touching" condition followed by a positive repulsive barrier which is more depleted the higher the KCl concentration. The deep negative part of the potential means that if two particles overcome the repulsive positive barrier they will aggregate irreversibly.

case, typical values of these parameters are $a \approx 30$ nm (obtained from scanning electron microscopy-SEM), $Z \approx 1000$, and $A_{eff}/k_BT \approx 60$ (for Ag colloids in water at room temperature). The accuracy of these parameters is questionable and, thus, so will be the potential they describe. Nevertheless, in the following we focus on aspects of the DLVO interaction potential that are present for a wide range of chosen parameter values.

Figure 1 shows the calculated interaction potential of two colloids for different ionicities according to the KCl concentration for the parameters given above. As can be seen, the repulsive potential barrier, V_{max}, varies greatly with salt concentrations in the range 5−20 mM. In particular, the barrier disappears for 20 mM. This correlates with our experimental observation on our silver colloids: a salt concentration of 20 mM collapses the sample completely and leaves (within an hour) a translucent liquid where all the colloids have collapsed by gravity in the form of large aggregates. This plot visualizes the well-known fact that colloid solutions quickly collapse even if the salt concentration only slightly exceeds a critical value,[1,3] for which $V_{max} < 0$.

Moreover, given the Boltzmann distribution of colloid energies one can deduce that aggregation can take place to a considerable extent even if the Coulomb potential barrier, V_{max}, exceeds room temperature by a few k_BT's (a typical minimum value to achieve stability is 15 k_BT). From the simplest point of view of the pair interaction potential in the DLVO theory, a positive potential barrier of a few k_BT's will not stop coagulation from occurring and it is only a matter of time before full aggregation occurs. Note, however, that the potential discussed here solely covers the interaction of two spheres, that is, dimer formation. It does not account for the interaction of more complex structures, which is precisely the point to achieve self-limiting aggregation by a Coulomb barrier, as explained in the next section.

III. Monte Carlo Simulations

We now want to address the following question based on the background discussion presented above: What is the aggregation dynamics of colloidal particles when the DLVO potential is close to the instability threshold, but still retains a positive repulsion barrier of a few k_BT's?

The question has an experimental motivation and is aimed at understanding the origin of the long-lived SERS active solutions we see in real samples, as we pointed out in the Introduction and as we shall show in the Experimental Section afterward.

Qualitatively, in rapid coagulation situations ($V_{max} < 0$), it is assumed that the aggregation process is driven mainly by the colloid dynamics (Brownian motion), because there is no potential barrier for collisions. This implicitly assumes that V_{max} remains negative for the interactions between larger structures, such as dimers, trimers, and so forth. One way to justify this is to assume that the interaction potential is additive, that is, the interaction of a colloid with a dimer is simply the sum of the interactions between this colloid and each of the two colloids forming the dimer. This then becomes a many-body problem, where the exact potential depends for example on the angle of approach of the colloid. For $V_{max} < 0$, this does not affect the aggregation too much because the attraction is never repulsive, for all cluster sizes. The situation could be very different when we are close to instability, that is, for $0 < V_{max} < 15\ k_BT$. The formation of dimer is then not negligible, and single colloids are not stable. It is likely, however, that the repulsive Coulomb hump for the interaction of a dimer and a colloid is larger than that for the pair interaction, say $2V_{max}$, and similarly for a trimer and a colloid, or two dimers. This implies that forming a cluster with two particles might be feasible if the barrier is a few k_BT's, but it will become less and less probable (exponentially) to add an additional particle to the cluster. This self-limiting aggregation of particles formally becomes a many-body problem in this context. The challenge is to show that in the presence of many particles (with clusters being approached by other clusters/particles from all possible directions and with different energies), small clusters remain stable for a sufficiently long time to become a state between the stable colloid and the fully aggregated situation. Metastability is, of course, a problem of definition of time-scales. A metastable colloidal state lasting for one year with an exponentially negligible probability of forming larger clusters becomes, for all practical purposes, a stable state.

Self-limiting aggregation of the sort described here can be demonstrated easily in a simplified Monte Carlo (MC) simulation. Hereby, a number of particles (with simplified interaction potentials) is initially distributed randomly over a finite Cartesian lattice. We show an example in two dimensions on a square lattice (200 × 200 sites) without loosing generality. A Metropolis algorithm alters the lattice particle configuration through a large number of Monte Carlo steps, whereby one iteration involves the following: (1) choosing a random particle; (2) calculating its potential energy, U_{ref}; (3) moving the particle to a randomly chosen neighboring position of the lattice; (4) calculating the particle's new potential energy, U; (5) if $U_{ref} \geq U$, the particle's move is accepted; and (6) for $U_{ref} < U$, the movement is only accepted with a certain probability given by a Boltzmann factor at a fixed temperature, T.

To model the repulsive Coulomb hump in the real DLVO-colloid potential close to the instability threshold, we choose the schematic potential shown in the inset of Figure 2. Essentially, two colloids separated by less than 1.5 lu (lattice units) become trapped in a very deep potential well ($V/k_BT < -40$). This includes the four nearest neighbors, and the four next nearest neighbors in a square lattice that are separated from

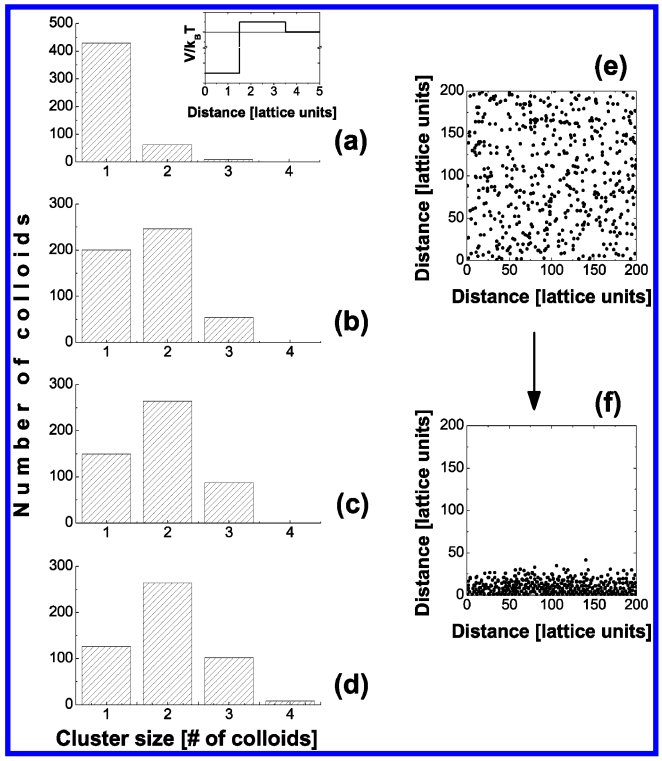

Figure 2. Monte Carlo simulation of self-limiting aggregation (square lattice 200 × 200, 500 particles, closed boundaries, Metropolis algorithm, positive Coulomb barrier with $V_{max}/k_BT = 10$). The "schematic DLVO-potential" with the qualitative features of the real potential, but adapted to a lattice, is shown in the inset of a. Parts a−d show the histograms of the number of particles participating in clusters of size 1, 2, 3, etc., after 10^6 MC steps in a, and then for an additional 5×10^7 MC iterations in each step from b−d. The predominance of *dimers* in the long term is a consequence of the particular choice of barrier height. To maximize the collision rate and interactions among clusters, we introduce a small asymmetry (1%) in the selection of the random movements in the Metropolis algorithm. After several million iterations this tends to accumulate the formed clusters toward a single boundary. This is shown in e and f where the initial (single particles) and the final (with small clusters) configurations are shown. This forces the clusters to interact among themselves and collapse into bigger clusters if they find the chance. The long-term survival of small clusters in this conditions is a demonstration of Coulomb-limited aggregation.

the reference site by $\sqrt{2}$ lu < 1.5 lu. The model potential then has a shallow positive hump ($V_{max}/k_BT \approx 1-10$, modeling the repulsive barrier before collapse in the DLVO theory) and then drops to zero for particles separated by more than 3.5 lu's.

The MC dynamics of aggregation of particles with a potential as shown in Figure 2 (that combines attractions and repulsions on different length scales) is extremely interesting and complex and would probably deserve a paper by itself. Here we content ourselves to the simplest facts for the purpose of this paper.

Figure 2a−d shows a series of histograms of the number of particles participating in clusters of size one (monomers), two (dimers), three (trimers), and so forth, for different MC running times. The simulation shown in Figure 2 was run for a positive repulsive hump of $V_{max}/k_BT = 10$. After 10^6 MC steps the sample still consists mainly of single particles, with a few dimers and a very small number of trimers. After an additional 5×10^7 MC steps dimers start dominating and become the dominant feature thereafter. Only after 10^8 further MC steps a very small number of tetramers appear for the first time; with the dimers being the dominant feature. The additive Coulomb barrier of the aggregated clusters makes it exponentially more difficult for further aggregation to occur. In fact, the *dominant type* of

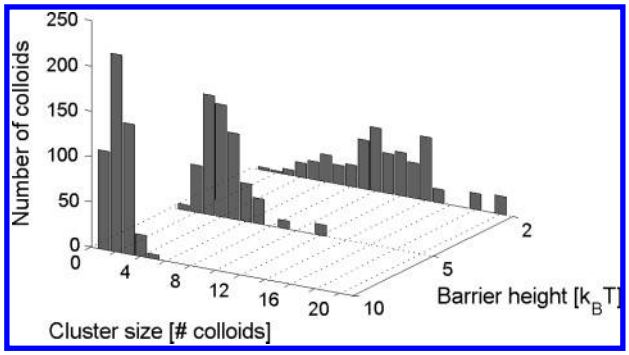

Figure 3. Monte Carlo simulation of self-limiting aggregation (square lattice 200 × 200, 500 particles, closed boundaries, Metropolis algorithm, positive Coulomb barriers of 2, 5, and 10 k_BT). The plot shows three histograms of the number of particles participating in clusters of size 1, 2, 3, etc, after 2×10^8 MC steps. Each histogram corresponds to a fixed potential; the barrier height is given on the *y* scale. The distribution of cluster sizes broadens and shifts to larger values for shallower repulsive barrier heights.

cluster in the final metastable state can be tuned by choosing different barrier heights or, alternatively, different temperature for a fixed barrier height. For a slightly lower barrier, trimers become the dominant feature after several million MC iterations, and so on. This correlation is depicted clearly in Figure 3. Here histograms of the number of colloids involved in different cluster types are shown for three different barrier heights. Each of the histograms corresponds to the resulting particle distribution after a 2×10^8 step MC simulation. Therefore, the histogram shown for the 10 k_BT barrier is an extension of the series of histograms shown in Figure 2a−d. For shallower barriers, the particle configuration noticeably shifts to larger clusters, that is, mainly trimers, tetramers, and pentamers for a 5 k_BT barrier and a broad distribution around decamers in the 2 k_BT case. In a real situation, the colloidal solution contains a variety of colloids with different sizes, shapes, surface charges, and therefore different interaction potentials. One would therefore expect a wider distribution of cluster sizes.

It should be noted that this phenomenon is solely due to Coulomb blocking of aggregation and not to a decrease in the collision rate. If all of the initial particles start forming dimers, then the density becomes smaller and the collision rate with other particles/clusters decreases accordingly. One could argue that the longer stability is precisely due to this decrease. To discard this possibility, we introduced a small imbalance (1%) in one direction (downward) in the choice of the random steps in the Metropolis algorithm. Besides simulating, in simplified terms, the effect of gravity, all single particles and clusters are forced to accumulate in the long run on the same side of the lattice and, therefore, are forced to interact and collide with one another all the time. This is illustrated schematically in Figure 2e−f where the initial (e) and final configurations (after 1.5×10^8 MC steps) are shown. Clusters (once formed and drifted toward the same place) have a very high collision rate with the others. The dominance of clusters with a typical size (dimers in the case of Figure 2d) is a manifestation of what we call here *self-limiting aggregation*.

We believe a state with self-limiting aggregation can explain both the high SERS activity of certain solutions and the long-term stability by the same token. We devote the next sections to an experimental proof supporting this point.

IV. Experiments

A. Samples and Methods. Raman/SERS spectra were measured in solution with a Jobin Yvon Raman spectrometer

(LabRam) coupled to a liquid N_2-cooled CCD detector and a confocal (Olympus BX2) microscope with an index-matched (water) × 100 (NA = 1) objective. Excitation was provided by a 633 nm CW HeNe laser (~3 mW at the sample).

Measurements were done on negatively charged Ag colloids, which were prepared according to the standard procedure described by Lee and Meisel.[22] The concentration of colloids in the base solution is estimated to be $\sim 10^{11}$ colloids/cm^3, based on the total Ag content and the average particle size measured by dynamic light scattering and observed in SEM. A benzotriazole dye (3-methoxy-4-(5′-azobenzotriazolyl)phenylamine), in the latter referred to as BTZ, which was specifically designed for SERS,[23] was used for most experiments (dye number 2 in ref 23). Later we also use Rhodamine 6G (RH6G) as an analyte. Unless stated otherwise, the number of dyes per colloid is ~1000.

Besides the spectroscopic information gained by SERS, scanning electron microscopy (SEM) was used on dried samples to image the typical aggregation state of the colloids. Dry samples were prepared as follows: a glass slide was covered with polylysine (1 mM) for 5 min, then rinsed with distilled water and left to dry. Next, a droplet of the sample to analyze was applied to the coated glass and left for 1 min, then rinsed and dried accordingly. Isolated clusters and/or single particles stick to the positively charged polylysine layer, leaving a representative population of the type of clusters/particles existing in the solution. This procedure avoids the possibility of additional aggregation, which would typically be induced if the colloidal solution was left to dry completely.

B. Build-Up and Origin of SERS Signals in Liquid. Our first task is to elucidate the origin of the SERS signals in liquid: single colloids or clusters. It is well known that the addition of a salt such as KCl is necessary to observe strong SERS signals. This would at first suggest that the signals originate from clusters, which aggregated as a result of salt addition. However, it is also possible that the main effect of KCl is chemical; that is, the chloride ions modify the silver surface in such a way that SERS signals are more enhanced. This could occur without colloid aggregation. The debate between the relative contributions of the chemical and electromagnetic enhancement in SERS is still ongoing.

If SERS comes from aggregates, then one expects to observe a build-up of the signal if we start from a sample with analyte but no KCl, and the salt is added at some specific point. Moreover, one should be able to see changes in the build-up of the signal according to the colloid concentration because particles should take longer/shorter to find each other depending on their density. Such a colloid concentration dependence should not occur if the effect is purely chemical (adsorption of chloride ions on the surface). In addition, the initial stages of the build-up ought to be well represented by the dynamics of dimer formation only, which is the most probable event at the beginning.

To study the build-up of the SERS signals as a function of colloid concentration we carried out in-situ measurements involving the following steps: (1) The base colloid solution was put in a small (~1 mL) disposable sample holder, and a SERS time-series measurement in immersion was started (1 s integration time) with the CCD detector centered conveniently in a region that would allow the spectrum of the dye to be monitored later. (2) After a few minutes (which yield the background SERS signal of the bulk solution), the BTZ dye was added to achieve the intended number of dyes per colloid. BTZ is known to adsorb strongly to Ag colloids by forming a covalent bond. Note that at the concentration used here (200 nM → ~1000 per colloid) this dye does not induce aggregation. The addition of BTZ provides the (weak) SERS signal without aggregation (single-particle enhancement regime). (3) Finally, a KCl solution was added to achieve the desired full SERS condition ($c_{KCl} = 10$ mM). This KCl concentration corresponds to about half of the concentration required for fast coagulation of the colloids. This is the regime of the onset of instability, as discussed in the previous sections. Following step 3, further Raman spectra were recorded for up to 2 h at intervals (dead time) of 1−1.5 s. We conducted three in-situ measurements based on bulk solutions with different colloid concentrations (bulk solution A: $\hat{c} \approx 10^{11}$ colloids/cm^3, B: $c = \hat{c}/2$, C: $c = \hat{c}/4$).

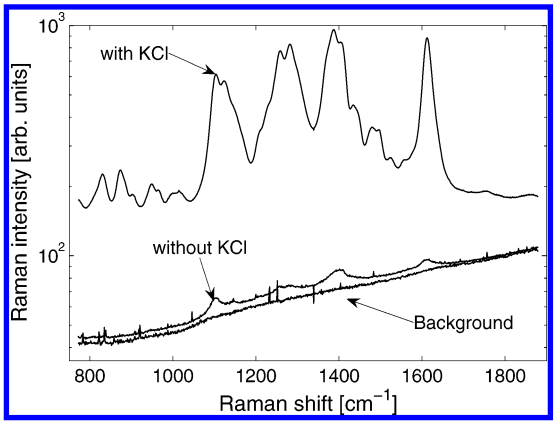

Figure 4. Averaged Raman/SERS spectra of sample C during the three in situ stages: pure colloid solution (background: average of 150 spectra), after addition of BTZ (without KCl: average of 750 spectra) and after addition of KCl (with KCl: average of 2300 spectra). Note the log-scale on the intensity axis.

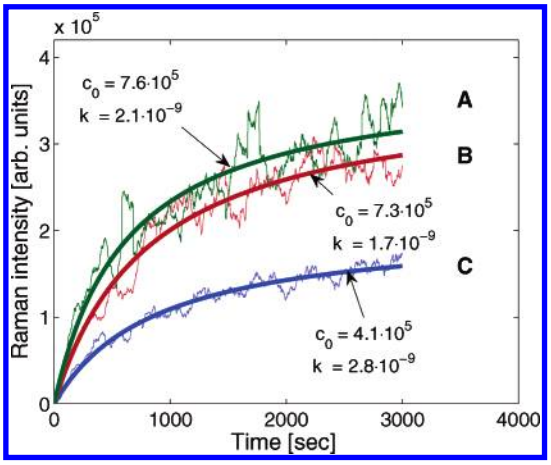

Figure 5. Build-up of the SERS signal (floating average with 50 spectra window size) for the samples with different initial colloid concentrations. Fits of eq 5 with the corresponding parameters are shown. A very good representation of the build-up is achieved even for sample A, where clustering beyond simple dimers in this time scale is known to occur. See the text for further details.

Figure 4 shows the average SERS signals over several minutes in the steady state of the three situations (colloid, colloid + dye, colloid + dye + KCl). Note the logarithmic scale in the figure and also note that SERS signals, although weak, can be seen in the liquid before aggregation.

The dynamics of the build-up of the signal is explicitly shown in Figure 5, where a floating average (window size 50 spectra) of the spectrally integrated Raman intensities of samples A, B, and C starting from the point of KCl addition- are plotted.

The first step of aggregation is two colloids forming one dimer, a process that will run with a rate constant, k, which depends on the positive potential barrier (Figure 1). Because two colloids need to be present in the same place, the process depends on the squared concentration of single colloids c_S; the dimer concentration c_P rises half as fast as c_S falls (to ensure colloid number conservation), that is

$$\frac{dc_S}{dt} = -kc_S^2, \qquad \frac{dc_P}{dt} = \frac{k}{2}c_S^2, \qquad c_S + 2c_P = c_S^{(0)} \quad (4)$$

The differential equations are trivial to integrate and lead to an expression for the time dependent dimer concentration, to wit

$$c_P(t) = \frac{c_S^{(0)}}{2}\left(\frac{c_S^{(0)}kt}{c_S^{(0)}kt + 1}\right) \quad (5)$$

where $c_S^{(0)}$ denotes the initial single colloid concentration. Given the enormous EM enhancement within a hot spot of a dimer and neglecting the possible formation of higher aggregates, we can assume that $I_{\text{Raman}} \propto c_P$; that is, this function is expected to be a good approximation to the Raman-signal build-up for low colloid concentrations.

In Figure 5, least-squares fits of eq 5 are shown (thick dashed lines) and the corresponding parameters displayed. The fits yield nearly equal rate constants, k, for the three different concentration regimes; this is expected because k depends only on the interaction potential, which is identical for samples A, B, and C (same c_{KCl}). The initial concentrations $c_S^{(0)}$ nearly reproduce the expected factor of 2 between samples B and C, but start having problems with the scaling for sample A. Obviously, the system of eq 4 is expected to be less and less accurate the higher the concentration because it fails to consider further clustering beyond dimers. Calculations of the electromagnetic enhancement of aggregates suggest that the enhancement factor does not scale with the number of colloids involved in a cluster. In fact, because the plasmon resonance of a cluster is known to show only few hot spots (due to the high selectivity with respect to the various conditions of the exciting EM field), higher aggregates are not expected to show a much stronger signal than dimers (i.e., in general I_{Raman} is not proportional to the number of colloids per cluster), which explains the apparently "reduced" initial concentrations $c_S^{(0)}$ for sample A.

Despite these shortcomings, it is quite clear that the dynamics of clustering, after screening of the Coulomb barrier, can be followed to a relatively good degree of accuracy both experimentally and theoretically. In the final steady state we achieve solutions that are highly SERS active, have a limited amount of clustering, and survive for several months without any deterioration in the signal level and concentration of clusters. This agreement strongly supports the fact that SERS signals originate mainly from clusters, with a large electromagnetic enhancement, rather than from single particles profiting from a large chemical enhancement.

Interestingly enough, the presence of these clusters does not have a dramatic, or sometimes even measurable, effect on the overall absorption spectrum of the solution. Clusters that produce very large SERS enhancements through the presence of hot spots do not necessarily have large contributions to the overall absorption; the SERS enhancement is only indirectly related to the absorption in general. If the state of aggregation of the colloid is much larger (either by increasing the salt or analyte concentration), then a tail of absorption can then be seen at long wavelengths; as reported, for example, in ref 24. This only happens, however, well beyond the metastable phase we describe here and the colloid is no longer stable over long periods of time, which is the interesting property we are trying to highlight in this study.

The exact nature of the clusters, however, cannot be decided by this experiment. Of particular interest for the present discussion is to clarify if the clustering is permanent (aggregation), temporary (reversible aggregation or flocculation), or simply dynamic pairing in which particles approach each other enough to produce a large SERS enhancement, but never actually bind with each other. These subtle aspects of the colloid dynamics (in the situation that is most favorable for SERS) have never been looked at in detail to the very best of our knowledge. A possibe approach to these problem is to look directly into a representative sample of clusters inside the liquid by SEM. This cannot be done in the liquid itself but can be done, with certain limitations, with the method of the polylysine substrates described in the Experimental Section and further expanded in the next subsection.

C. Electron Microscopy. The polylysine coated glass acts as a "glue" that captures a small fraction of the clusters existing in the colloidal solution and immobilizes them for further inspection once the sample is dry. This collection of captured clusters is expected to be a faithful representation of the situation in the liquid, accordingly. SEM images of the different mixture stages (pure colloids (pC), colloids with 10 mM KCl (CK), and colloids with both KCl and the BTZ dye added (CKB)) were taken to prove their state of aggregation. All samples are coated immediately before the SEM with a 5 nm layer of platinum to increase the quality of the SEM images by avoiding excessive charging by the electron beam.

There is a compromise in the amount of time the polylysine substrate is exposed to the solution to obtain a representative sampling of clusters. The longer the time, the larger the number of clusters that can be observed and the better the statistics we can get from them, but the more we increase the chances of "accidental clustering" on the surface. A one minute exposure followed by rinsing seems to be a good compromise between the two.

Excerpts of the resulting images are shown in Figure 6. As expected, we observed single colloids and a tiny fraction of dimers in the case of pC. For CK, on the contrary, we estimated that ca. one-third of the colloids had aggregated, forming small clusters of various types. The large polydispersity of clusters observed here, compared to the theoretical predictions of Section III is attributed to the polydispersity of the colloids in the starting solution. The results observed for CKB are similar to those of CK. We were not able to observe further aggregation or a qualitative difference induced by BTZ, meaning that at 200 nM dye concentration the overall balance of charge is not dominated by the dye but rather by stabilizing citrate ions.

These results demonstrate the existence of limited clustering in these solutions. The SEM images for the sample with KCl and dye + KCl have been obtained from sample A in the previous subsection, in which clustering beyond simple dimers is expected.

The presence of clusters in these images suggests that dynamic pairing/collisions is not the main origin of the SERS signals. Still, neither the results presented in this subsection nor the ones in the previous one exclude the possibility of reversible aggregation as the cause for the long-term stability of these liquids. The images presented here are snapshots of the population of clusters inside the liquid at the time the clusters

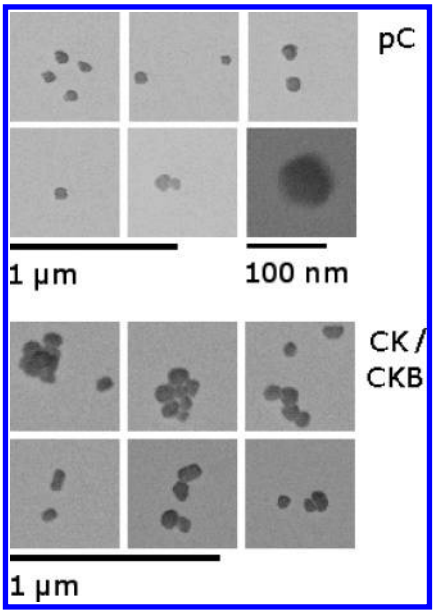

Figure 6. Excerpts from SEM images of pure colloids (pC), colloids with KCl (CK), and colloids with KCl + BTZ (CKB) at various magnifications. Note that for pC a few dimers can be found, although they are very rare. The single Ag colloids (one of which shown in full magnification) match very well the average expected size deduced from dynamic light scattering (DLS), which is ~60 nm in diameter. In the case of CK and CKB, various types of small clusters intersperse the images. These clusters are very common and demonstrate the existence of limited aggregation in the solution. The CK and CKB examples are shown together because their SEM results were indistinguishable. Adding the BTZ dye at 200 nM concentration makes no measurable difference as far as the shape and average size of the clusters is concerned.

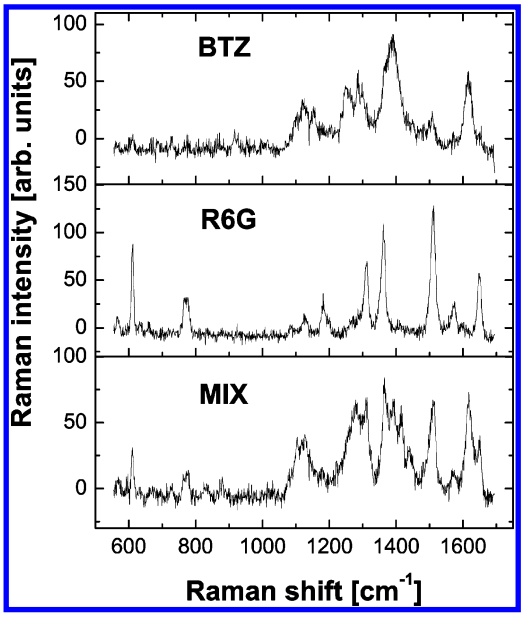

Figure 7. Three independent spectra extracted from the total scan of (D + E) of 2000 spectra with 0.2 s integration time each. These three events correspond essentially to pure RH6G- or BTZ-like events, or a mixed event where spectral features of both dyes can be clearly identified. By fitting each spectrum with eq 6, and using the averaged intensities in the pure samples, the (normalized) relative contributions of each dye given by eq 7 can be obtained.

hit the polylysine film, but they do not say much about their long-term stability. The results of the next subsection are designed to clarify this point and show that aggregation here is irreversible and, therefore, further clustering is being avoided by Coulomb repulsion and not by an equilibrium process between clustered and free particles (reversible coagulation or flocculation).

D. Stability of the Aggregates. The questions we try to address in this section are the following: Are the small aggregates stable like the ones found in the MC-simulations? Are they permanently aggregated or is there a finite equilibrium constant between aggregated and free particles which maintains the long term stability? These are questions that are not easily answered experimentally. As pointed out before, many SERS experiments can be interpreted by either a permanent or dynamic aggregation of particles.

A possible way out of this is to study SERS spectra for mixtures of two samples using two analytes, as we shall show in this subsection. Raman spectra of SERS samples (colloid concentration $\hat{c}$, salt $c_{KCl} = 10$ mM) with two Raman active probe compounds, BTZ and RH6G (100 nM each), were recorded (samples D and E, respectively). Both samples are left for a few hours to let aggregation take place and achieve a steady state of SERS activity. First, the SERS intensities of both samples were measured with long integration times; this is to be used later as reference spectra to account for the different Raman cross sections of both dyes. Subsequently, both samples were mixed together (D + E) and a measurement of 2000 spectra with 0.2 s integration time each was started immediately.

The *average spectra* (over the whole run) of the mixed D + E sample matches the sum of both reference spectra within expected experimental errors. Hence, for each spectra we can assume to see a weighted sum of the reference spectra:

$$I_{mix}(\nu) = \alpha I^{ref}_{BTZ}(\nu) + \beta I^{ref}_{RH6G}(\nu) + B \qquad (6)$$

where α and β are weighting factors and B takes into account a constant background value (which are normally inevitable under SERS conditions). For full analysis, each Raman spectrum of D + E was decomposed according to this function by means of a least-squares fitting algorithm. From the parameters α and β one can deduce the partial contribution (p) of each dye to each spectrum

$$p_{BTZ} = \frac{\alpha}{\alpha + \beta}, \qquad p_{RH6G} = \frac{\beta}{\alpha + \beta} \qquad (7)$$

As time evolves we monitor signals (with 0.2 s integration time each) with varying intensities that look either more RH6G-like, more BTZ-like, or a mixture of both. This is shown explicitly in Figure 7 where three independent spectra have been isolated from the total scan of 2000 spectra.

We now correlate the intensity of the events with the dye fractions defined in eq 7. Most interesting are the events with the highest intensities. The reason is as follows: spectra with signatures of both dyes can come from events in which there was more than one type of cluster within the scattering volume of the objective within the integration time. However, the largest signals come from a situation where the coupling to a specific cluster was optimized by chance and we are seeing the dye content of a specific hot spot within a cluster.

If aggregation is irreversible, then a hot-spot on a given cluster will contain one type of dye only, depending on whether this cluster was formed in solution D or E. On the contrary, if aggregation is a reversible and dynamic process, then clusters from D and E will break up and form new clusters containing both types of dye. In the first case one expects all high-intensity events to be composed of the signal of one dye only, whereas in the latter case some high-intensity events could show a mixed

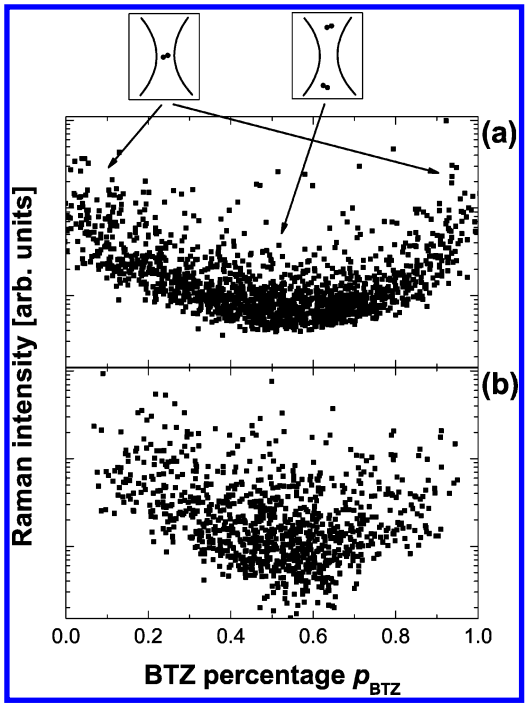

Figure 8. Plot a shows the correlation plot of intensity vs dye concentration (p_{BTZ}) for the mixed D + E sample. For comparison, a correlation plot of a slightly different sample is shown in b, as opposed to D + E where both dyes were mixed *before* exposure to colloids during sample preparation. All other sample conditions (concentrations etc.) were kept constant. Note the log-scale in the intensity axes. See the text for further details.

signal. The situation would then be similar to the case where aggregates are formed first and dyes are added together.

Figure 8a shows the correlation plot between the intensity of the spectra and the BTZ dye fraction (a similar plot can be done for the RH6G fraction). The intensities of pure BTZ or RH6G are normalized by the average intensity in the pure samples to account for the different Raman efficiencies of both. The "banana" shape in Figure 8a has the following meaning: In the statistical sense, whenever the intensity is very high (i.e., coming principally from one cluster only) the signal is either a pure BTZ or pure RH6G event. The vast majority of events with mixed signals are low in intensity, meaning that they were events where more than one cluster was present (without maximum coupling to the laser) in the scattering volume.

If aggregation was reversible and dynamic to keep the long-term stability of the solution, we should see after several hours high-intensity events coming from single clusters with both RH6G and BTZ. This is, in fact, the case if *both* dyes are added together to a colloid solution with the appropriate KCl concentration; as opposed to adding them separately and then mixing the solutions once the clusters have been formed. As can be seen in Figure 8b, if the dyes are added together, the "banana" shape of the correlation plot in Figure 8 is lost, and a cone-shaped correlation cloud is obtained, which does *not* yield the high-intensity dye-selectivity of the former experiment.

The correlation plot in Figure 8a remains unaltered after several days, which demonstrates that aggregation in the small clusters is irreversible and that further aggregation and long-term stability must be the consequence of Coulomb interactions rather than a dynamic equilibrium or reversible aggregation.

We believe that all of the experimental evidence gathered in the last three subsections points toward the existence of a stable (or metastable over very long periods of time) state in these colloids where limited aggregation in small clusters blocks further collapse by Coulomb repulsion. This is exactly the same scenario found in Monte Carlo simulations for particles with a simplified version of the DLVO potential.

V. Conclusions

We have shown theoretical and experimental evidence for a metastable state with limited aggregation of particles very close to the instability threshold in metallic colloids. Besides its interest from a purely colloid-science standpoint, its long-term stability and limited aggregation makes it ideal for the monitoring of analytes in SERS and any other spectroscopic techniques that profit from collective surface plasmon excitations in small clusters. The phenomenon of self-limiting aggregation by Coulomb repulsions is very interesting by itself and comes from a partially screened two-particle DLVO potential in combination with the correlations among particles in the aggregation process. From a simple practical viewpoint (in terms of SERS), the stability of the partially aggregated phase should provide solutions with long-term usability, where reproducibility and statistical analysis can be performed with increased confidence and better control.

Acknowledgment. Special thanks are due to David Flynn (Victoria University of Wellington) for help with the electron microscopy and to Kate McGrath (Victoria University of Wellington) for a critical reading of the manuscript. P.G.E. acknowledges partial support for this work by the Engineering and Physical Sciences Research Council (EPSRC) of the U.K. under grant GR/T06124.

References and Notes

(1) Fennell Evans, D.; Wennerström, H. *The Colloidal Domain*; Wiley-VCH: New York, 1999.
(2) Varis, K.; Mattila, M.; Arpiainen, S.; Ahopelto, J.; Jonsson, F.; Sotomayor Torres, C. M.; Egen, M.; Zentel, R. *Opt. Express* **2005**, *13*, 2653.
(3) Hunter, R. J. *Foundations of Colloid Science*; Clarendon Press: Oxford, 1989; Vols. I and II.
(4) Derjaguin, B. V.; Landau, L. *Acta Physicochim. URSS* **1941**, *14*, 633.
(5) Verwey, E. J.; Overbeek, J. *Theory of the Stability of Lyophobic Colloids*; Elsevier: Amsterdam, 1948.
(6) Trizac, E.; Raimbault, J. *Phys. Rev. E* **1999**, *60*, 6530.
(7) Crocker, J. C.; Grier, D. G. *Phys. Rev. Lett.* **1996**, *77*, 1897.
(8) Dobnikar, J.; Rzehak, R.; von Grünberg, H. H. *Europhys. Lett.* **2003**, *61*, 695.
(9) Dobnikar, J.; Chen, Y.; Rzehak, R.; von Grünberg, H. H. *J. Phys.: Condens. Matter* **2003**, *15*, 263.
(10) Grier, D. G. *J. Phys. Condens. Matter* **2000**, *12*, A85.
(11) Moskovits, M.; Vlcková, B. *J. Phys. Chem. B* **2005**, *109*, 14755.
(12) Fleischmann, M.; Hendra, P. J.; McQuillan, A. J. *Chem. Phys. Lett.* **1974**, *26*, 163.
(13) Jeanmaire, D. L.; Van Duyne, R. P. *J. Electroanal. Chem.* **1977**, *84*, 1.
(14) Albrecht, M. G.; Creighton, J. A. *J. Am. Chem. Soc.* **1977**, *99*, 5215.
(15) Moskovits, M. *Rev. Mod. Phys.* **1985**, *57*, 783.
(16) Otto, A. In *Light Scattering in Solids*; Cardona, M., Güntherodt, G., Eds.; Springer: Berlin, 1984; p. 289.
(17) Nie, S.; Emory, S. R. *Science* **1997**, *275*, 1102.
(18) Kneipp, K.; Wang, Y.; Kneipp, H.; Perelman, L. T.; Itzkan, I.; Dasari, R. R.; Feld, M. S. *Phys. Rev. Lett.* **1997**, *78*, 1667.
(19) Etchegoin, P.; Cohen, L. F.; Hartigan, H.; Brown, R. J. C.; Milton, M. J. T.; Gallop, J. C. *J. Chem. Phys.* **2003**, *119*, 5281.
(20) Etchegoin, P.; Cohen, L. F.; Hartigan, H.; Brown, R. J. C.; Milton, M. J. T.; Gallop, J. C. *Chem. Phys. Lett.* **2004**, *383*, 577.
(21) Pailthorpe, B. A.; Russel, W. B. *J. Colloid Interface Sci.* **1982**, *89*, 563.
(22) Lee, P. C.; Meisel, D. *J. Phys. Chem.* **1982**, *86*, 3391.
(23) Graham, D.; McLaughlin, C.; McAnally, G.; Jones, J. C.; White, P. C.; Smith, W. E. *Chem. Commun.* **1998**, *11*, 1187.
(24) Faulds, K.; Littleford, R. E.; Graham, D.; Dent, G.; Smith, W. E. *Anal. Chem.* **2004**, *76*, 592.